Proc. Natl. Acad. Sci. USA
Vol. 82, pp. 8458–8462, December 1985
Biophysics

Active site dynamics of ribonuclease

(enzyme kinetics/protein dynamics/solvation/stochastic boundary simulation/water structure)

AXEL T. BRÜNGER, CHARLES L. BROOKS III*, AND MARTIN KARPLUS

Department of Chemistry, Harvard University, Cambridge, MA 02138

Contributed by Martin Karplus, August 15, 1985

ABSTRACT **The stochastic boundary molecular dynamics method is used to study the structure, dynamics, and energetics of the solvated active site of bovine pancreatic ribonuclease A. Simulations of the native enzyme and of the enzyme complexed with the dinucleotide substrate CpA and the transition-state analog uridine vanadate are compared. Structural features and dynamical couplings for ribonuclease residues found in the simulation are consistent with experimental data. Water molecules, most of which are not observed in crystallographic studies, are shown to play an important role in the active site. Hydrogen bonding of residues with water molecules in the free enzyme is found to mimic the substrate–enzyme interactions of residues involved in binding. Networks of water stabilize the cluster of positively charged active site residues. Correlated fluctuations between the uridine vanadate complex and the distant lysine residues are mediated through water and may indicate a possible role for these residues in stabilizing the transition state.**

Bovine pancreatic ribonuclease A is an ideal system for a theoretical study of the structural and dynamic basis of enzyme catalysis. Although little is known about the physiological role of ribonuclease, a particularly wide range of biochemical, physical, and crystallographic data are available for this enzyme (1, 2). These have led to proposals for the catalysis of the hydrolysis of RNA by a two-step mechanism (3), in which a cyclic phosphate intermediate is formed and subsequently hydrolysed. Both steps are thought to involve in-line displacement at the phosphorus and to be catalyzed by the concerted action of a general acid and a general base. In spite of the accumulated experimental information, a full understanding of the mechanism and a detailed analysis of the rate enhancement produced by ribonuclease has not been achieved. One approach for supplementing the available experimental data is provided by molecular dynamics simulations. Such simulations are particularly useful for exploring aspects of the active site dynamics that are difficult to characterize by other techniques.

To achieve a realistic treatment of the solvent-accessible active site of ribonuclease, a new molecular dynamics simulation method has been implemented. It makes possible the simulation of a localized region, approximately spherical in shape, that is composed of the active site with or without ligands, the essential portions of the protein in the neighborhood of the active site, and the surrounding solvent. The approach provides a simple and convenient method for reducing the total number of atoms included in the simulation, while avoiding spurious edge effects. Using this method we have performed molecular dynamics simulations of the solvated active site of ribonuclease A, ribonuclease A with the dinucleotide substrate CpA, and ribonuclease A with the transition-state analog uridine vanadate (UVan). Analysis of the simulation provides new insights concerning the interactions between ligands and active site residues and permits elucidation of the role of water in stabilizing the structure and charges of the active site.

METHODS

The stochastic boundary molecular dynamics simulation method (4–6) for solvated proteins uses a known x-ray structure as the starting point; for the present problem we have made use of the refined high-resolution (1.5 to 2 Å) x-ray structures kindly provided by G. Petsko and co-workers (7, 8); the CpA structure was built from the crystal results for dCpA by introducing the 2′ oxygen into the deoxy sugar. The region of interest (here the active site of ribonuclease A) is defined by choosing a reference point (which is taken at the position of the phosphorus atom in the CpA complex) and constructing a sphere of 12 Å radius around this point. Space within the sphere not occupied by crystallographically determined atoms is filled by water molecules, introduced from an equilibrated sample of liquid water. A picture of the portion of the protein and the solvent included in the simulation is shown in Fig. 1. The 12 Å sphere is further subdivided into a reaction region (10 Å radius) treated by full molecular dynamics and a buffer region (the volume between 10 and 12 Å) treated by Langevin dynamics, in which Newton's equations of motion for the non-hydrogen atoms are augmented by a frictional term and a random-force term; these additional terms approximate the effects of the neglected parts of the system and permit energy transfer in and out of the reaction region. Water molecules diffuse freely between the reaction and buffer regions but are prevented from escaping by an average boundary force (5). The protein atoms in the buffer region are constrained by harmonic forces derived from crystallographic temperature factors (6). The forces on the atoms and their dynamics were calculated with the CHARMM program (9); the water molecules were represented by the ST2 model (10). The entire system for each simulation was equilibrated for 12 psec; this involved thermalization of the component atoms and adjustment of the number of waters in the active site region to obtain the normal liquid density in regions distant from the protein. After equilibration, 27 psec of simulation was performed for each of the three systems; it is the results of these simulations that are reported here. Details of the methodology and additional results will be given elsewhere.

RESULTS AND DISCUSSION

The behavior of the individual simulations and their comparison provide a number of insights into aspects of the active site region of ribonuclease that are important for an understanding of substrate binding and catalysis. Fig. 2*a* shows a

The publication costs of this article were defrayed in part by page charge payment. This article must therefore be hereby marked "*advertisement*" in accordance with 18 U.S.C. §1734 solely to indicate this fact.

Abbreviation: UVan, uridine vanadate.

*Present address: Department of Chemistry, Carnegie-Mellon University, Pittsburgh, PA 15213.

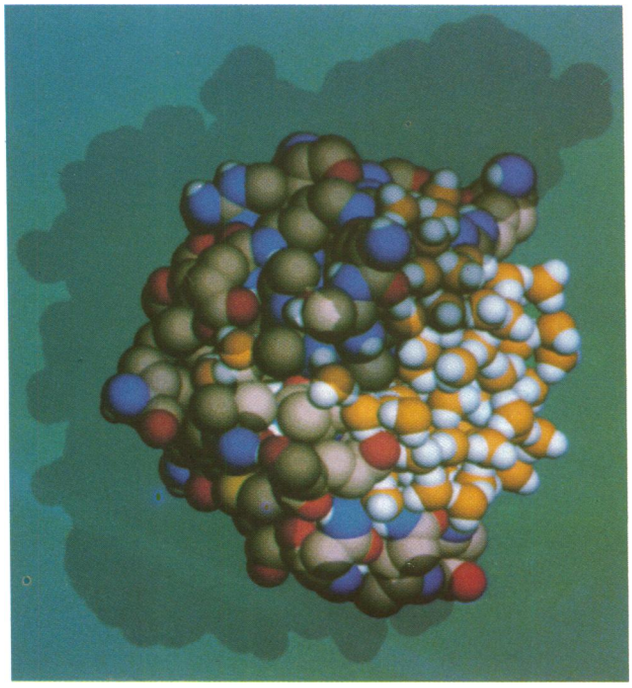

FIG. 1. Active site region of aqueous ribonuclease A within stochastic boundary; shown is a space-filling representation of the van der Waals spheres of protein and water atoms included in the stochastic boundary molecular dynamics simulation. The structure is obtained from a "snapshot" at 15 psec after equilibration. The shaded regions indicate the parts of the molecule that have been eliminated in the simulation (see text).

stereo picture of the average dynamics structure for ribonuclease, in the absence of substrate or other anions (sulfate, phosphate) bound to the active site (8). Residues that have been implicated in substrate binding (Thr-45 and Ser-123 in the "pyrimidine" site and Gln-69, Asn-71, and Glu-111 in the "purine" site) and in catalysis (His-12 and -119; Lys-7, -41, and -66; Phe-120, Asp-121, and Gln-11) are shown, with some additional residues that may be involved in maintaining the integrity of the active site; the average positions of water molecules are included. In what follows, we shall examine first the native results in the absence of bound anions and then compare them with those obtained in the presence of CpA and UVan.

One of the striking aspects of the active site of ribonuclease is the presence of a large number of positively charged groups, some of which may be involved in guiding and/or binding the substrate (11). The simulation demonstrated that these residues are stabilized in the absence of ligands by well-defined water networks. A particular example is shown in Fig. 3, which includes Lys-7, -41, and -66, Arg-39, and the doubly protonated His-119, as well as the water molecules within 3 Å of any charged site with their energetically most likely hydrogen bonds. The bridging waters, some of which are organized into trigonal bipyramidal structures, are able to stabilize the otherwise very unfavorable configuration of positive groups because the interaction energy between water and the charged $C\text{-}NH_n^+$ ($n = 1, 2$, or 3) moieties is very large; e.g., at a donor–acceptor distance of 2.8 Å, the $C\text{-}NH_3^+\text{–}H_2O$ energy is −19 kcal/mol with the empirical potential used for the simulation (9), in approximate agreement with accurate quantum mechanical calculations (ref. 12; unpublished data) and gas-phase ion-molecule data (13). The average energy stabilization of the charged groups (Lys-7, -41, and -66, Arg-39, and His-119) and the 106 water molecules included in the simulation is −376.6 kcal/mol. This energy is calculated as the difference between the simulated system and a system composed of separate protein and bulk water. Unfavorable protein–protein charged-group interactions are balanced by favorable water–protein and water–water interactions. The average energy per molecule of pure water from an equivalent stochastic boundary simulation (5) is −9.0 kcal/mol, whereas that of the waters included in the active site simulation is −10.2 kcal/mol; in the latter a large contribution to the energy comes from the interactions between the water molecules and the protein atoms. It is such energy differences that are essential to a correct evaluation of binding equilibria and the changes introduced by site-specific mutagenesis (14).

During the simulation, the water molecules involved in the charged-group interactions oscillate around their average positions, generally without performing exchange. On a longer time scale, it is expected that the waters would exchange and that the side chains would undergo larger-scale displacements. This is in accord with the disorder found in the x-ray results for lysine and arginine residues (e.g., Lys-41 and Arg-39; see refs. 7 and 15), a fact that makes difficult a crystallographic determination of the water structure in this case. Water stabilization of charged groups has been observed (16, 17) or suggested (18) in other proteins. It is also of interest that Lys-7 and Lys-41 have an average separation of only 4 Å in the simulation, less than that found in the x-ray structure. That this like charged pair can exist in such a configuration is corroborated by experiments that have shown that the two lysines can be crosslinked (19); the structure of this compound has been reported recently (20) and is similar to that found in the native protein.

In addition to the role of water in stabilizing the charged groups that span the active site and participate in catalysis, water molecules make hydrogen bonds to protein polar groups that become involved in ligand binding. A particularly clear example is provided by the adenine-binding site in the CpA simulation (Fig. 2*b*). The NH_2 group of adenine acts as a donor, making hydrogen bonds to the carbonyl of Asn-67, and the ring N^{1A} acts as an acceptor for a hydrogen bond from the amide group of Glu-69 (see Table 1). Corresponding hydrogen bonds are present in the free ribonuclease simulation, with appropriately bound water molecules replacing the substrate. These waters and those that interact with the pyrimidine-site residues Thr-45 and Ser-123 (see below) help to preserve the protein structure in the optimal arrangement for binding. Similar substrate "mimicry" has been observed in x-ray structures of lysozyme (21) and of penicillopepsin (22). The presence of such waters in the active site has the consequence that water extrusion and its inverse must be intimately correlated with substrate binding and product release; e.g., there are 23 fewer waters in the active site of the CpA complex than for free ribonuclease in the present simulation.

A selected list of strong hydrogen bonds in the various x-ray and average dynamics structures is given in Table 1. Most of the interactions are similar in the crystal and simulated structures. Binding interactions in the pyrimidine-binding site are indicated by hydrogen bonds between Thr-45 and the cytidine (uridine) base in the CpA (UVan) complex. Comparisons of the x-ray structures of uridine and cytidine base inhibitor complexes (23) suggest that Ser-123 may be important for the binding of uridine. In the UVan simulation, Ser-123 shows persistent hydrogen bonding interaction with the uridine base complex (see Fig. 2*c*), whereas in the x-ray structure of Gilbert *et al.* (7), no bond between Ser-123 and the uridine base is indicated (see Table 1). Stabilization of the cytidine base in the dinucleotide substrate may also occur through perpendicular stacking interactions with Phe-120, as is apparent in Fig. 2*b* and in the x-ray structure (7). This type of interaction, which corresponds to that found in benzene

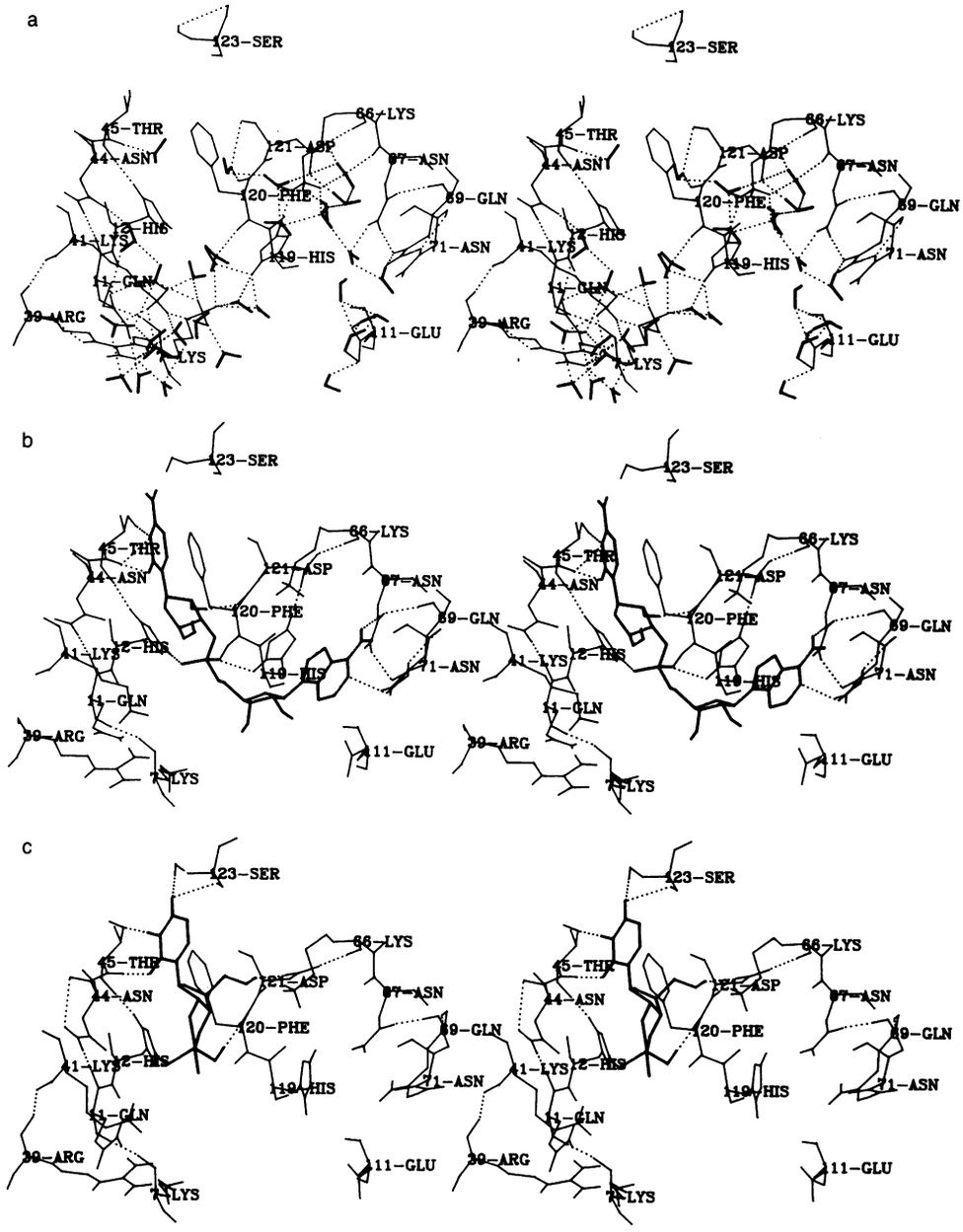

FIG. 2. (*a*) Stereo drawing of native ribonuclease A including active site residues and bound water molecules. The structure corresponds to the molecular dynamics average structure of the protein and water molecules. Protein·protein hydrogen bonds are indicated when the heavy donor–acceptor distance is less than 3.5 Å and the donor–hydrogen–acceptor angle is less than 65.0°. (b) Similar to *a*, for the ribonuclease–CpA complex, including substrate and active site residues. (*c*) Similar to *a*, for the ribonuclease–UVan complex, including substrate and active site residues.

crystals (24), has been discussed recently for proteins (25). His-12 forms a strong hydrogen bond via $N^{\epsilon 1}$ to the carbonyl of Thr-45 and is found to be relatively immobile and similarly positioned in all three structures. By contrast, His-119 is considerably more mobile and has different orientations in the various structures. Specifically, there is a hydrogen bond from $N^{\epsilon 2}$ to Asp-121 in the CpA complex but not in either of the other dynamics average structures; in the free ribonuclease simulation, His-119 participates in the water network already described. Also, His-119 undergoes dihedral-angle transitions in some of the simulations. This greater freedom of His-119, relative to His-12, which may be important for the catalytic mechanism, is in accord with the alternative conformations found in some x-ray structures (23, 26). In none

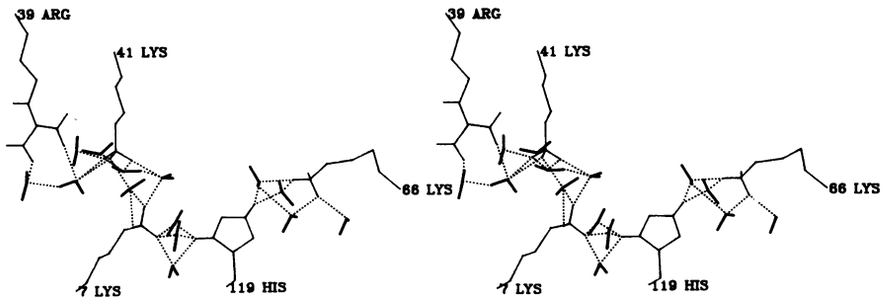

FIG. 3. Stabilization of positively charged groups by bridging water molecules in the active site of native ribonuclease A without anions. The stereo drawing corresponds to a snapshot of the molecular dynamics trajectory at 15 psec. The picture includes only the residues Lys-7, Arg-39, Lys-41, Lys-66, and His-119 and the bound water molecules. The hydrogen-bonding criteria are the same as used in Fig. 2.

Table 1. Comparison of hydrogen bonds in x-ray structures and in molecular dynamics (MD) average structures

Hydrogen bond		Distance,* Å					
		RNase		RNase–CpA		RNase–UVan	
Donor	Acceptor	x-ray	MD	x-ray	MD	x-ray	MD
His-12 ($N^{\delta 1}$)	Thr-45 (O)	2.8	2.7	2.7	2.9	2.6	2.6
Lys-66 (N)	Asp-121 ($O^{\delta 2}$)	2.8	2.8	2.7	2.8	3.0	2.8
His-119 ($N^{\epsilon 2}$)	Asp-121 ($O^{\delta 1}$)	2.8	—	2.7	2.6	—	—
His-12 ($N^{\epsilon 2}$)	CpA (O^{2})			3.2	2.8		
Lys-41 (N^{ζ})	CpA (O^{2})			2.8	—		
Thr-45 (N)	CpA (N^{3C})			—	3.4		
Thr-45 (N)	CpA (O^{2C})			2.8	2.7		
Thr-45 ($O^{\gamma 1}$)	CpA (N^{3C})			—	2.9		
Gln-69 ($N^{\epsilon 2}$)	CpA (N^{1A})			3.4	3.0		
Asn-71 ($N^{\epsilon 2}$)	CpA (N^{1A})			3.3	—		
His-119 ($N^{\delta 1}$)	CpA (O^{1})			3.2	2.8		
Phe-120 (N)	CpA (O^{1})			2.9	3.1		
CpA (N^{6A})	Asn-67 ($O^{\delta 1}$)			—	3.3		
CpA (N^{6A})	Asn-71 ($O^{\delta 1}$)			3.1	—		
CpA ($O^{2'C}$)	Phe-120 (O)			—	2.7		
His-12 ($N^{\epsilon 2}$)	UVan (O^{8})					2.6	—
His-12 ($N^{\epsilon 2}$)	UVan (O^{1})					—	2.7
Thr-45 (N)	UVan (O^{2})					2.8	2.7
Phe-120 (N)	UVan (O^{8})					2.9	—
Ser-123 (N)	UVan (O^{4})					—	3.5
Ser-123 (O^{γ})	UVan (O^{4})					—	2.8
UVan (N^{3})	Thr-45 ($O^{\gamma 1}$)					2.6	2.7
UVan (O^{8})	Phe-120 (O)					—	2.6
UVan ($O^{5'}$)	Asp-121 ($O^{\delta 1}$)					—	2.8

Selected hydrogen bonds for the residues and substrates shown in Fig. 2 *a–c*; the criteria for the existence of a hydrogen bond are the same as in Fig. 2: the donor–acceptor distance has to be <3.5 Å and the donor–hydrogen–acceptor angle <65°.
*Between the donor and the acceptor atoms.

of the simulations do His-12 and His-119 get closer to each other than 5 Å; in the free ribonuclease simulation, they are separated by three water molecules. This confirms the suggestion of Campbell and Petsko (8), based on the x-ray structure, that the Witzel mechanism (27), which postulates a direct interaction between the two histidines, is not tenable.

In both the dCpA x-ray structure and the CpA simulation, $N^{\epsilon 2}$ of His-12 is coupled to O^{2} of the phosphate group (which is also hydrogen-bonded to two water molecules in the simulation) but is still well-positioned to interact with the 2′ hydroxyl of the sugar. $N^{\delta 1}$ of His-119 is bonded to O^{1} of the phosphate, as is the main-chain N of Phe-120 in both the x-ray and the simulation structure. For UVan, His-12 is in a similar position and the $N^{\epsilon 2}$ group is hydrogen bonded to O^{8} of the pentacoordinate vanadate. It is clear that His-12 moves to follow the negatively charged group of UVan which is displaced relative to that in CpA; such a "tracking" motion is also noted in ref. 7. His-119, which interacts with the $O^{5'}$ side chain of the sugar of UVan, has intervening water molecules between it and the vanadate ion, in accord with its role as a general base in the hydrolysis step of the reaction. In the x-ray structure (7) and the neutron structure (28), His-119 is somewhat closer to the vanadate group than in the simulation. As to Lys-41, neither in the x-ray structure (it is disordered) nor in the dynamic structure is it bonded to CpA. In the UVan complex, the crystal structure shows a direct interaction between the N^{ζ} groups of Lys-41 and O^{2} of vanadate, whereas the dynamic structure shows a somewhat longer-range interaction with O^{1}. The reduced mobility for Lys-41 in the x-ray and neutron structures may originate from the use of a vanadate complex in the experiment; in the simulation, the smaller atomic charges appropriate for a phosphate group, rather than vanadate, were employed, and the Lys-41 mobility is only slightly less in the UVan complex than in the free enzyme. Lys-7 is displaced toward the ligand on CpA and UVan binding, relative to the free enzyme, but has no direct interactions with the ligands in either case.

In the x-ray structure of the substrate analog dCpA (7), it was noted that the dinucleotide is in a *gauche, trans* configuration that would permit stereoelectronic assistance in phosphodiester hydrolysis (29). During the simulation, the phosphate backbone undergoes a transition to the more stable *gauche, gauche* configuration (30), where it remains for the remainder of the time. The significance of this transition requires further investigation, particularly because it may be related to the interaction with His-12 (see above), which is in the doubly protonated imidazolium ion form observed in the neutron crystal study. A singly protonated imidazole species is required for it to act as a general base in the catalytic mechanism. NMR measurements of the histidine protonation state (28) under the same conditions as in the neutron study suggest that His-12 and -119 are both present as a mixture of singly and doubly protonated species, although only the latter is observed in the crystal. Since the hydrogen-bonding behavior of the two protonation states is expected to be different, additional simulations need to be done to fully elucidate the role of the histidine residues (e.g., CpA with His-12 singly protonated and His-119 doubly protonated).

To supplement the positional results concerning important interactions obtained from the average structure, it is important to introduce *dynamical* information pertaining to the motions of different groups. This provides an indication of transient short-range interactions and longer-range correlated motions that may be important in interpreting chemical events but are not evident in the static average structure. The magnitudes of the correlated fluctuations between the atomic displacements of the protein and the ligand, relative to the dynamics average structure, are shown for the CpA and UVan complexes in Fig. 4 *a* and *b*, respectively. Although the time scale of the simulation is short compared with the observed rate constants, it is important to remember that the actual catalytic event in a given molecule occurs on a picosecond time scale. The overall time scale of the reaction can be orders of magnitude longer due to the fact that a reaction is rare, not that it is slow. Many of the large correlations (positive or negative) correspond to atoms in close

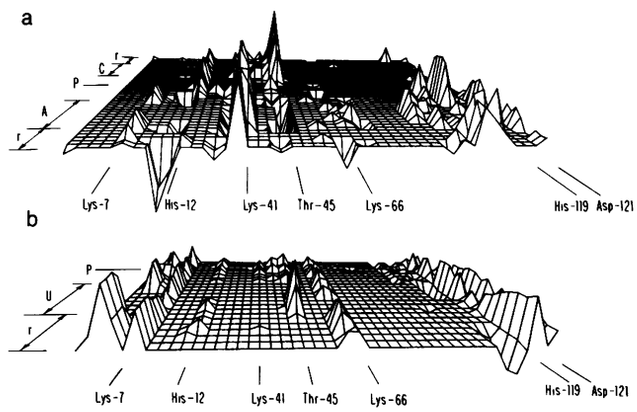

FIG. 4. (*a*) Normalized cross-correlations of the atomic fluctuations of the ribonuclease–CpA complex; only correlations with absolute values greater than 0.3 are shown, and an averaging over all atoms within each protein residue was performed. The 45 residues included in the simulation as well as in the drawing are Glu-2, Thr-3, Ala-4, Ala-5, Ala-6, Lys-7, Phe-8, Glu-9, Arg-10, Gln-11, His-12, Met-13, Met-30, Arg-33, Leu-35, Arg-39, Lys-41, Pro-42, Val-43, Asn-44, Thr-45, Phe-46, Val-47, Val-54, Cys-65, Lys-66, Asn-67, Asn-71, Cys-72, Gln-69, Cys-84, Ile-106, Ile-107, Val-108, Ala-109, Cys-110, Glu-111, Val-116, Pro-117, Val-118, His-119, Phe-120, Asp-121, Ala-122, and Ser-123 (in consecutive order, note the disconnectivities). r, Ribose ring atoms. (*b*) Same as *a*, for the ribonuclease–UVan complex.

proximity; an example is the correlation of Thr-45 and the pyrimidine, which have strong hydrogen-bonding interactions. His-119 has strong correlations with the phosphate group in CpA and the vanadate group in UVan; the latter is of particular interest because there are at least two water molecules, on the average, between the imidazole ring and the phosphate group. An analogous case is Asp-121, which has strong correlations with the substrate in both the CpA and the UVan complex; in the latter Asp-121 is hydrogen-bonded to the CH_2OH group of the sugar, but in the former it is coupled indirectly through His-119 and Phe-120. Lys-7 and -66 both are correlated significantly with the UVan ligand, although the N^{ζ} groups of the two lysines are more than 5 Å removed in both cases. The dynamic coupling appears to be mediated by an intervening water network, whose structural role was described above. By contrast Lys-41, which interacts directly with the vanadate group, shows only a very weak correlation. However, the results of a new simulation (unpublished data) of the cyclic cytidine monophosphate transition-state analog indicate a strong correlation between Lys-41 and the cyclic phosphate group. Such correlated fluctuations between the distant lysine residues and the phosphate group of the substrate may indicate a possible role for the lysine residues in stabilizing the transition state.

To further characterize catalysis by ribonuclease A, dynamical studies of substrate binding and product release, as well as of structural changes that occur along the reaction pathway, are required. Also, a detailed treatment of the reaction dynamics by activated dynamics techniques (31) is needed.

We are grateful to G. A. Petsko for making the x-ray coordinates available to us and for stimulating discussions of the results. We thank A. Wlodawer for kindly providing the neutron coordinates of the UVan complex. We have profited from discussions with L. C. Allen. A.T.B. wishes to thank W. Bode, G. M. Clore, A. M. Gronenborn, R. Huber, D. Oesterhelt, J. W. Pflugrath, and W. Steigemann for assistance during his stay at the Max-Planck-Institute for Biochemistry (Martinsried, F. R. G.). C.L.B. wishes to thank the National Institutes of Health for postdoctoral support. This work has been supported in part by a grant from the National Science Foundation.

1. Richards, F. M. & Wyckhoff, H. W. (1971) in *The Enzymes*, ed., Boyer, P. D. (Academic, New York), 3rd Ed., Vol. 4, pp. 647–907.
2. Blackburn, P. & Moore, S. (1982) in *The Enzymes*, ed., Boyer, P. D. (Academic, New York), 3rd Ed., Vol. 15, pp. 317–433.
3. Roberts, G. C. K., Dennis, E. A., Meadows, D. H., Cohen, J. S. & Jardetzky, O. (1969) *Proc. Natl. Acad. Sci. USA* **62**, 1151–1158.
4. Brooks, C. L. & Karplus, M. (1983) *J. Chem. Phys.* **79**, 6312–6323.
5. Brünger, A., Brooks, C. L. & Karplus, M. (1984) *Chem. Phys. Lett.* **105**, 495–500.
6. Brooks, C. L., Brünger, A. & Karplus, M. (1985) *Biopolymers* **24**, 843–865.
7. Gilbert, W. A., Fink, A. L. & Petsko, G. A. (1986) *Biochemistry*, in press.
8. Campbell, R. L. & Petsko, G. A. (1986) *Biochemistry*, in press.
9. Brooks, B. R., Bruccoleri, R. D., Olafson, B. O., States, D. J., Swaminathan, S. & Karplus, M. (1983) *J. Comp. Chem.* **4**, 187–217.
10. Stillinger, F. H. & Rahman, A. (1974) *J. Chem. Phys.* **60**, 1545–1557.
11. Matthew, J. B. & Richards, F. M. (1982) *Biochemistry* **21**, 4989–4999.
12. Desmeules, D. J. & Allen, L. C. (1980) *J. Chem. Phys.* **72**, 4731–4748.
13. Kebarle, P. (1977) *Annu. Rev. Phys. Chem.* **28**, 445–476.
14. Fersht, A. R., Shi, J.-P., Knill-Jones, J., Lowe, D. M., Wilkinson, A. J., Blow, D. M., Brick, P., Carter, P., Waye, M. M. Y. & Winter, G. (1985) *Nature (London)* **314**, 235–238.
15. Wlodawer, A. (1985) in *Biological Macromolecules and Assemblies: Volume 2–Nucleic Acids and Interactive Proteins*, eds., Jurnak, F. A. & McPherson, A. (Wiley, New York), pp. 394–439.
16. Baker, E. N. & Hubbard, R. E. (1984) *Prog. Biophys. Mol. Biol.* **44**, 97–179.
17. Sawyer, L. & James, M. N. G. (1982) *Nature (London)* **295**, 79–80.
18. Tabushi, I., Kiyosuke, Y. & Yamamura, K. (1981) *J. Am. Chem. Soc.* **103**, 5255–5257.
19. Marfey, P. S., Uziel, M. & Little, J. (1965) *J. Biol. Chem.* **240**, 3270–3275.
20. Weber, P. C., Salemme, F. R., Lin, S. H., Konishi, Y. & Scheraga, H. A. (1985) *J. Mol. Biol.* **181**, 453.
21. Blake, C. C. F., Pulford, W. C. A. & Artymiuk, P. J. (1983) *J. Mol. Biol.* **167**, 693–723.
22. James, M. N. G. & Sielecki, A. R. (1983) *J. Mol. Biol.* **163**, 299–361.
23. Borkakoti, N., Moss, D. S. & Palmer, R. A. (1982) *Acta Crystallogr. Sect. B* **38**, 2210–2217.
24. Wyckoff, R. W. G. (1969) *The Structure of Benzene Derivatives*, (Interscience, New York).
25. Burley, S. K. & Petsko, G. A. (1985) *Science* **229**, 23–28.
26. Borkakoti, N. (1983) *Eur. J. Biochem.* **132**, 89–94.
27. Witzel, H. (1963) *Prog. Nucleic Acid Res. Mol. Biol.* **2**, 221–258.
28. Borah, B., Chen, C.-W., Egan, W., Miller, M., Wlodawer, A. & Cohen, C.-W. (1985) *Biochemistry* **24**, 2058–2067.
29. Gorenstein, D. G., Findlay, J. B., Luxon, B. A. & Kar, D. (1977) *J. Am. Chem. Soc.* **99**, 3473–3479.
30. Alagona, G., Ghio, C. & Kollman, P. A. (1985) *J. Am. Chem. Soc.* **107**, 2229–2239.
31. Northrup, S. H., Pear, M. R., Lee, C.-Y., McCammon, J. A. & Karplus, M. (1982) *Proc. Natl. Acad. Sci. USA* **79**, 4035–4039.